RESEARCH ARTICLE

Pneumonia initiates a tauopathy

Ron Balczon[1,2] | Mike T. Lin[2,3] | Ji Young Lee[2,3,4] | Adeel Abbasi[5] |
Phoibe Renema[2,3] | Sarah B. Voth[2,3] | Chun Zhou[2,3] | Anna Koloteva[2,3] |
C. Michael Francis[2,3] | Neel R. Sodha[6] | Jean-Francois Pittet[7] |
Brant M. Wagener[7] | Jessica Bell[2,3] | Chung-Sik Choi[2,3] | Corey E. Ventetuolo[5,8] |
Troy Stevens[2,3,4]

[1]Department of Biochemistry and Molecular Biology, University of South Alabama, Mobile, AL, USA

[2]Center for Lung Biology, University of South Alabama, Mobile, AL, USA

[3]Department of Physiology and Cell Biology, College of Medicine, Center for Lung Biology, University of South Alabama, Mobile, AL, USA

[4]Internal Medicine, University of South Alabama, Mobile, AL, USA

[5]Pulmonary, Critical Care and Sleep Medicine, Department of Medicine, Alpert Medical School of Brown University, Providence, RI, USA

[6]Department of Surgery, Brown University, Providence, RI, USA

[7]Department of Anesthesiology and Perioperative Medicine, School of Medicine, The University of Alabama at Birmingham, Birmingham, AL, USA

[8]Health Services, Policy and Practice, Brown University School of Public Health, Providence, RI, USA

Correspondence
Corey E. Ventetuolo, Pulmonary, Critical Care and Sleep Medicine, Department of Medicine, Alpert Medical School of Brown University, Rhode Island Hospital, Providence, RI 02912, USA.
Email: corey_ventetuolo@brown.edu

Troy Stevens, Department of Physiology and Cell Biology, College of Medicine, Center for Lung Biology, University of South Alabama, Mobile, AL 36688, USA.
Email: tstevens@southalabama.edu

Abstract

Pneumonia causes short- and long-term cognitive dysfunction in a high proportion of patients, although the mechanism(s) responsible for this effect are unknown. Here, we tested the hypothesis that pneumonia-elicited cytotoxic amyloid and tau variants: (1) are present in the circulation during infection; (2) lead to impairment of long-term potentiation; and, (3) inhibit long-term potentiation dependent upon tau. Cytotoxic amyloid and tau species were recovered from the blood and the hippocampus following pneumonia, and they were present in the extracorporeal membrane oxygenation oxygenators of patients with pneumonia, especially in those who died. Introduction of immunopurified blood-borne amyloid and tau into either the airways or the blood of uninfected animals acutely and chronically impaired hippocampal information processing. In contrast, the infection did not impair long-term potentiation in tau knockout mice and the amyloid- and tau-dependent disruption in hippocampal signaling was less severe in tau knockout mice. Moreover, the infection did not elicit cytotoxic amyloid and tau variants in tau knockout mice. Therefore, pneumonia initiates a tauopathy that contributes to cognitive dysfunction.

THE **FASEB** JOURNAL

1 | INTRODUCTION

Lower respiratory tract infections afflict ~280 million people and account for 2.38 million deaths worldwide, on an annual basis.[1,2] This high prevalence of infections includes both bacterial and viral causes of pneumonia. In addition, more than 177 million cases of SARS-CoV-2 infection have been documented to date. Many of these patients present with dyspnea, gas exchange abnormalities and varying degrees of pneumonia.[3-5] While pneumonia represents an important cause of acute respiratory failure, it also leads to chronic and debilitating illness in survivors, with high rates of morbidity and mortality.[6-8] Patients who survive from these infections exhibit unusually high rates of cognitive dysfunction that can persist, for reasons that are unknown.[9-18]

Recent studies have revealed that pneumonia elicits the endothelial production of cytotoxic amyloid and tau variants within the lung. The amyloid and tau cytotoxins can be found in the airway[19,20] and in the cerebrospinal fluid[20,21] during an infection. In the lung, they promote exudative edema and hinder repair from injury. In the brain, they acutely impair hippocampus long-term potentiation (LTP), and over time, they decrease LTP, spine density and memory acquisition.[20-22] Whether cytotoxic amyloid and tau variants access the circulation during infection as a mechanism for distribution to the brain, whether the blood-borne species impair hippocampal long-term potentiation in the absence of infection, and whether they rely upon tau for their cytotoxicity is unknown. Here, we test the hypothesis that pneumonia elicits blood-borne cytotoxic tau variants, and that tau is necessary for the infection to impair hippocampal information processing.

2 | MATERIALS AND METHODS

2.1 | Animals

Experimentation with animals was approved by the Institutional Animal Care and Use Committee of the University of South Alabama and conducted according to the "Guide to the Care and Use of Laboratory Animals."

2.2 | Rats

Adult 10- to 12-week-old CD rats weighing ~300-350 g were used in this study (Charles River Laboratories). Rats were anesthetized using a ketamine/xylazine mixture (80/5 mg/kg body weight). After a surgical plane was achieved and confirmed by the absence of a toe pinch reflex, the ventral neck was shaved, and hair removed using a cream, then the area was cleaned and disinfected with chlorhexidine. Using sterile instruments, an ~2.5 cm incision was made through the skin, the underlying cervical fascia was retracted and the external muscles blunt dissected to expose the trachea. The surgical table was lifted to 90°. Either bacteria (PA103Δ*exoUexoT::Tc* pUCP*exoY*; ExoY$^+$) or amyloids in 200 µL saline were insufflated into the airway using a 27-gauge needle, immediately under the thyroid gland. After the needle was removed and hemostasis was confirmed, the skin was sutured using sterile 3.0 silk and the surgical site cleaned with chlorhexidine. Animals were moved into a recovery cage and after recovery from anesthesia they were moved to a dedicated room in the vivarium. Animals were checked daily.

A concentration of 10^{7-8} ExoY$^+$ was used for these studies, based upon prior experience using this mutant. Animals were monitored during recovery from anesthesia and were provided with food and water ad libitum. Terminal surgeries were performed 24 hours, 48 hours, and 1 mo following bacterial and amyloid inoculations. During the terminal surgery animals were anesthetized using isoflurane (1%-3%) while cardiac and pulmonary ultrasound analysis was performed. Anesthesia was then increased to achieve a surgical plane (3%-4%). An incision was made in the abdomen and the stomach and intestines were externalized to enable isolation of the abdominal aorta. A 24-gauge × ¾ inch catheter was placed in the abdominal aorta and blood was drawn to a volume of 8-12 mL. Blood was placed in a heparin tube and centrifuged, plasma was collected, and plasma was frozen for later amyloid isolation and Western blotting. Organs were harvested, including the heart, lungs and brain, flash-frozen in liquid nitrogen and saved for Western blotting. The hippocampus was isolated and split into two hemispheres, where half of the brain was prepared for electrophysiological recordings and the other half was used for western blotting.

2.3 | Mice

Adult 9- to 13-week-old wild type (C57BL/6J) and tau knockout (B6.129S4(Cg)-$Mapt^{tm1(EGFP)/Klt}$/J, Stock No: 029219; The Jackson Laboratory, Bar Harbor, ME) mice were used. For primary infection studies, mice were anesthetized by intraperitoneal injection of a ketamine/xylazine mixture (80/5 mg/kg of body weight) and inoculated intratracheally with ExoY$^+$ (10^5 CFU in 40 μL) or saline vehicle (40 μL). At 48 hours after the infection, brain and plasma (~0.5-1 mL) were collected immediately after euthanasia. Hippocampal slices prepared from the brains were used for LTP studies, and circulating tau was purified from the plasma.

Tau purified from mouse plasma was desalted into 40 μL of saline and the total amount was injected either through the trachea or tail vein, as indicated. Hippocampal LTP was recorded at 48 hours post-injection.

Green fluorescence in B6.129S4(Cg)-$Mapt^{tm1(EGFP)/Klt}$/J mice can be visualized to identify tau-expressing cells. To determine whether lung capillary endothelium expresses tau, tomato lectin (LEL, TL Dylight 649; Vector lab. #DL-1178) and NucBlue (Hoechst nuclear dye; Invitrogen) were infused into the circulation. Gelatin was introduced into the circulation and agarose was introduced into the airway, as described previously.[23] The lung was then cut into 300 μm sections and imaged by confocal microscopy.[23]

2.4 | Bacterial preparation for inoculation

ExoY$^+$ from a frozen stock was cultured overnight on Vogel-Bonner agar supplemented with 400 μg/mL carbenicillin. Bacteria were harvested into sterile PBS (10 mL), vortexed, and centrifuged (6000 g for 10 minutes). Following centrifugation, the supernatant was discarded, and the pellet was resuspended in 1 mL of sterile PBS. The optical density of this suspension was measured at 540 nm (OD$_{540}$) using a spectrophotometer. The bacterial inoculation was prepared at a concentration of 10^{7-8} colony forming units (CFUs) per 200 μL in rats, or 10^5 per 40 μL for inoculation in mice, using the previously established conversion ratio where an OD$_{540}$ of 0.25 represents 2×10^8 CFUs/mL.[24-26]

2.5 | Echocardiography

A Vevo 3100 (VisualSonics, Toronto, ON, Canada) with a 30 MHz transducer (MX550D) was used to evaluate cardiac and pulmonary function. Spontaneously breathing rats were anesthetized with isoflurane 1.5% (titrated as needed) in a 1:1 O$_2$–air admixture. Heart rate, electrocardiogram, and respiration were continuously recorded using the sensor-embedded exam pad, while cardiac and pulmonary ultrasound parameters were assessed, as described in detail previously.[27]

2.6 | Sarkosyl precipitation of tau

Sarkosyl-insoluble tau was precipitated from tissue homogenates and plasma using methods similar to those outlined by Kanaan et al.[28] Brains and hearts were weighed and then suspended in 3× weight per volume of homogenization buffer composed of 50 mM Tris, pH 7.4, 274 mM NaCl, 5 mM KCl, 1 mM phenylmethylsulfonyl fluoride and 1 μg/mL each of chymostatin, leupeptin, antipain, and pepstatin. The organs were homogenized with 30 strokes of a Dounce homogenizer, and the homogenate was centrifuged at 14 000 g for 40 minutes at 4°C. The supernatant was retained on ice, and the pellets were resuspended in a volume equivalent to the starting volume with a buffer composed of 10 mM Tris, pH 7.4, 800 mM NaCl, 10% sucrose, 1 mM ethylene glycol-bis(2-aminoethyl) tetraaceticacid, 1 mM phenymethylsulfonyl fluoride (resuspension buffer), and then homogenized and centrifuged as outlined above. The supernatant from this second centrifugation was added to the initial supernatant, sarkosyl was added from a 20X stock to a final concentration of 1%, and the samples were incubated at 37°C for 60 minutes. The samples were then centrifuged in a SW40 rotor at 27 500 rpm for 3 hours. The pellets were suspended in 200 μL of the resuspension buffer and stored at −80°C until analyses via immunoblotting. To precipitate tau from plasma and extracorporeal membrane oxygenation (ECMO) oxygenator eluates, either 1.5 mL of plasma or 10 mL of ECMO eluate was diluted 1:1 with resuspension buffer, sarkosyl was added to 1%, and the preparations were incubated and centrifuged as outlined above.

2.7 | Immunoblot analysis

Immunoblotting was performed using methods that we described previously in detail.[20,21] T22 anti-oligomeric tau antibody (EMD Millipore Corp., Temecula, CA, product #ABN454) was used at a dilution of 1:5000 and peroxidase-labeled anti-rabbit secondary antibody (Abcam, Cambridge, UK, product #ab7090) was used at a dilution of 1:20 000. Blots were developed using chemiluminescence procedures according to the manufacturer's recommended procedures (Thermo Scientific, Rockford, IL, product #A38554).

2.8 | Immuno-isolation of amyloid and tau species

Amyloid and tau variants were immuno-isolated using methods we have detailed previously.[20,21] For these studies, 1 μL each of T22 anti-oligomeric tau and A11 anti-amyloid oligomer (StressMarq Biosciences, Victoria, BC, product #SPC-506 or Invitrogen, Rockford, IL, product #AHB0052) antibodies were added to either 1.5 mL of rat plasma, 200 μL mouse plasma, or 10 mL of ECMO oxygenator eluates, and the mixtures were incubated with shaking overnight at 4°C. The next morning, 75 μL protein A-agarose (Santa Cruz Biotech, Dallas, TX, product #sc-2001) was added and the mixture was incubated at room temp for 3 hours with shaking. The beads were collected by pelleting, washed 6× with borate saline buffer (BSB; Teknova, Inc, Hollister, CA, product #B0230), once with BSB containing 0.5 M NaCl, once with BSB containing 0.05% Tween 20, and then amyloids were eluted by addition of BSB containing 4 M $MgCl_2$. The beads were pelleted, and the supernatant containing amyloids was collected and placed at 100°C for 15 minutes to denature any eluted antibodies. The isolated heat-stable amyloids then were desalted into HBSS (Gibco, Grand Island, NY, product #14025-092) using a micro-concentrator device with a 3 kDa cut-off (Merck Millipore, Darmstadt, Germany, product #UFC800324). The isolated rat plasma and ECMO oxygenator isolated amyloids were suspended to 600 μL in HBSS and 200 μL of the preparation was intratracheally administered to three different rats. The amyloids that were isolated from mouse plasma were suspended in 120 μL BSB and 40 μL of the preparation was intratracheally administered to three different mice.

2.9 | Hippocampal slice preparation

Hippocampal slices were prepared similarly from rats and mice. Upon obtaining the brains from the rodents after euthanasia, the brains were submerged in an ice-cold sucrose-artificial cerebrospinal fluid (in mM): 70 sucrose, 80 NaCl, 2.5 KCl, 21.4 $NaHCO_3$, 1.25 NaH_2PO_4, 0.5 $CaCl_2$, 7 $MgCl_2$, 1.3 ascorbic acid, and 20 glucose. After 1 minute incubation, the cerebral cortices were removed, and the hippocampi were placed onto an agar block, transferred into a slicing chamber (Leica VT1200s, Leica Instruments), and the prepared transverse hippocampal slices (300 μm) were placed in a holding chamber containing regular artificial cerebrospinal fluid (in mM): 125 NaCl, 2.5 KCl, 21.5 $NaHCO_3$, 1.25 NaH_2PO_4, 2.0 $CaCl_2$, 1.0 $MgCl_2$, and 15 glucose. Slices were incubated at 35°C for 30 minutes and then at room temperature for 1 hour before field potentials were recorded at room temperature. All solutions were constantly equilibrated with carbogen (95% O_2 and 5% CO_2).

2.10 | Electrophysiology recordings

Hippocampal slices were visualized using a fixed-stage upright microscope (Leica) equipped with infrared differential interference contrast optics. The recording chamber was continuously superfused (1 mL/min) with artificial cerebrospinal fluid containing SR95531 (2 μM) and CGP55845 (1 μM) to block inhibitory synaptic transmission. Both recording and stimulating electrodes were pulled from borosilicate glass pipettes (BF150-86-10; Sutter Instruments), and when filled with artificial cerebrospinal fluid, had tip resistance of 1 and 0.6 MΩ, respectively. The stimulating electrode, connected to an ISO-Flex stimulus isolation unit (AMPI), was placed in the CA1 stratum radiatum (150 and 100 μm from the somata of rat and mouse hippocampi, respectively) to stimulate the CA3 axon collaterals. CA3 region was cut away to eliminate recurrent excitation within the CA3 subfield. Stimulus duration was 0.1 ms, allowing for clear separation of fiber volley from the preceding stimulus artifact.

Recordings were obtained using an EPC10 amplifier (HEKA). Analog signals were further amplified 10× and filtered at 5 kHz using an Axopatch amplifier (Axon Instrument) and digitized at 20 kHz using Patchmaster software (HEKA). Evoked field excitatory postsynaptic potentials were recorded every 20 seconds. Following a stable field excitatory postsynaptic potential baseline of >10 minutes, a theta-burst stimulation, consisting of three sweeps (a single burst consists of five stimuli delivered at 100 Hz and ten bursts delivered at 5 Hz per sweep) delivered at 30 seconds intervals, was delivered to induce synaptic strengthening. Long-term potentiation was calculated from 55 to 60 minutes post the theta-burst stimulation and normalized to the baseline field excitatory postsynaptic potential.

2.11 | ECMO study cohort

This study was approved by the Institutional Review Board at the ECMO center (Rhode Island Hospital; IRB #221618). Oxygenators (Maquet Quadrox HLS 7.0, Getinge, Germany) from 11 patients supported with ECMO were included. For this study, oxygenators from consecutive patients supported with either a veno-venous (VV) or veno-arterial (VA) configuration and regardless

of etiology were included. Clinical care was not altered for the purposes of this study. Following decannulation, the oxygenators were packaged without any treatment or manipulation and shipped to the laboratory for analysis. Demographic and clinical characteristics of patients were extracted from the electronic health record. Pneumonia was retrospectively defined by AA, who was blinded to the cytotoxicity results, as evidence of clinical suspicion documented by the treating intensive care unit team with a confirmed culture (sputum, bronchoalveolar lavage or viral respiratory panel) within seven days of initiating ECMO or while on circuit up to the day of decannulation.[29]

2.12 | Cytotoxicity assay

Upon their receipt, de-identified oxygenators (ie, laboratory staff were blinded to all clinical data) were flushed with 480 mL of HBSS containing calcium and magnesium; residual blood together with the HBSS was considered to be membrane oxygenator effluent. The membrane oxygenator effluent was centrifuged (2500 g for 10 minutes), separated into aliquots, and then frozen for future use. At the time of the experiment, membrane oxygenator effluent was thawed, filter-sterilized (0.22 μm), heated to 37°C, and then incubated on confluent monolayers of pulmonary microvascular endothelial cells for 24 hours. Effluent cytotoxicity was assessed by quantifying inter-endothelial cell gap formation and lactate dehydrogenase (LDH) release into the supernatant.[20,21]

2.13 | Isolation of amyloid proteins from ECMO oxygenators

To assess whether oligomeric tau was present in the membrane oxygenator effluent, a T22-based ELISA was developed. In this ELISA, T22 immunoreactivity was tested in the membrane oxygenator effluent. To compare the relative cytotoxicity of membrane oxygenator effluent to the endothelial cell infection bioassay, either PA103 or ExoY$^+$ were incubated on endothelial cells. The infection(s) caused progressive endothelial gap formation over 4-6 hours and release of oligomeric tau. The supernatant collected after the experiment was stored at −80°C. This supernatant was thawed and applied to cells in the absence of bacteria. Infection-derived supernatant caused severe cytotoxicity, an effect that is largely abolished by neutralization with the T22 antibody.[20,21] Undiluted and serially diluted supernatant was tested for T22 immunoreactivity, and this result was directly compared to the results obtained with membrane oxygenator effluents. Because the oligomeric tau produced by

endothelium following infection is heat-stable, samples were also boiled at 100°C for 30 minutes and the T22 immunoreactive signal re-assessed.[19]

2.14 | Data and statistical information

Offline data analysis and statistical comparison were performed using custom macros written in Igor Pro (WaveMatrics) and Prism (GraphPad). Field excitatory postsynaptic potential amplitude was determined from the peak, and the slope was measured between 10% and 50% of the rising phase. Data were binned at 1 minute and 2 minutes intervals to generate summary field excitatory postsynaptic potential amplitude and slope plots, respectively. Data are expressed as mean ± SD or SEM and statistically compared as specified, where $P < .05$ was denoted as statistically significant.

3 | RESULTS

3.1 | Lung infection initiates a proteopathy

Pseudomonas aeruginosa (PA103Δ*exoUexoT::Tc* pUCP*exoY*; ExoY$^+$) was introduced into the airways of rodents (Figure 1A).[24-26] Twenty-four and 48 hours following infection, cardiac and pulmonary ultrasonography was performed, blood was drawn from the abdominal aorta, and the hippocampus was isolated for measurement of LTP. Ultrasound revealed a hyperdynamic circulatory state with increased left ventricular ejection fraction (Figure 1B) and a heterogeneous pattern of lung injury with multi-focal areas of hyperechoic vertical B lines (Figure 1C). Sarkosyl extraction of the plasma, heart, and brain tissues followed by immunoblotting for oligomeric tau revealed increased T22 immunoreactivity in all three organ systems (Figure 1D), consistent with infection-dependent production of oligomeric tau. Electrophysiological recordings at the hippocampal Schaffer synapses demonstrated normal LTP at 24 hours and impaired LTP at 48 hours (Figure 1E); representative electrophysiological traces are shown in Figure S1A. Thus, *P aeruginosa* lung infection leads to an increase in T22 immunoreactive tau within the plasma and hippocampus, coincident with suppressed LTP.

Next, we collected A11- and T22-immunoreactive amyloid and tau variants, respectively, from 3% of the plasma volume of animals harboring infection for 48 hours (Figure 2A).[19-21] In control experiments, these antibodies were tested in uninfected animals.
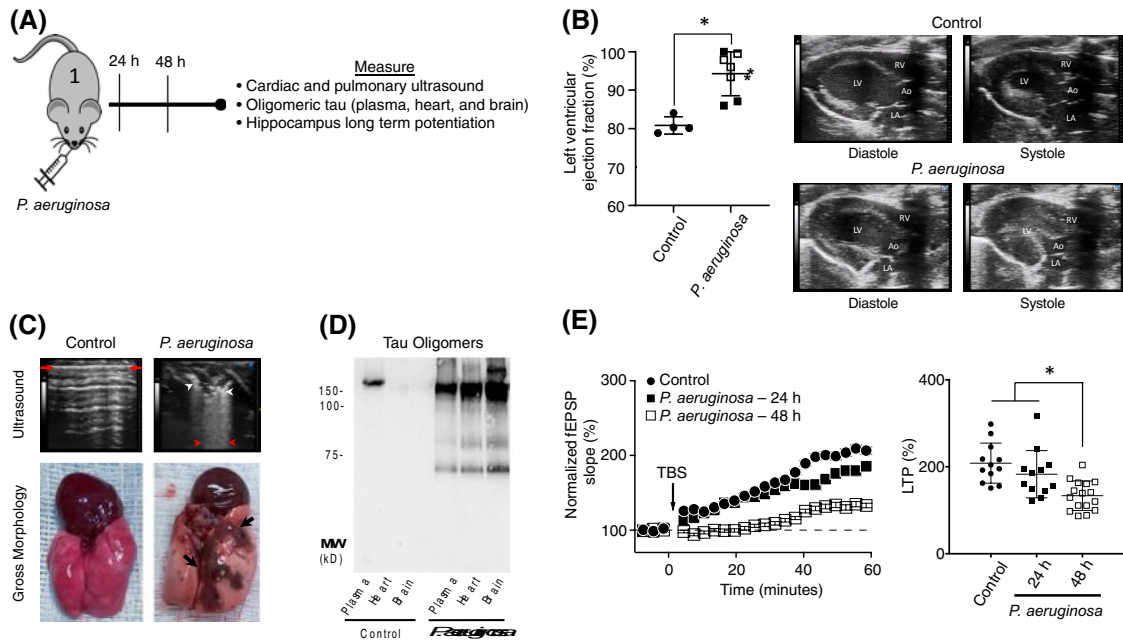
FIGURE 1 Pneumonia elicits a hyperdynamic circulatory state coincident with tau oligomer distribution to peripheral organs and suppressed long-term potentiation. A, *P aeruginosa* was introduced directly into the airway of animals and peripheral organ function was tested 24 and 48 hours later. This primary infection is designated by a "1". B, *P aeruginosa* increased left ventricular ejection fraction at 24 hours (closed squares) and 48 h (open squares) post-infection, characteristic of a hyperdynamic circulatory state ($P = .002$ using Student's t-test; left-hand panel). Data represent mean $\pm$ SD. Representative ultrasound images of diastole and systole in the long axis parasternal view are shown in control and infected animals (right-hand panel). Ao = aorta; LA = left atrium; LV = left ventricle; RV = right ventricle. C, Representative ultrasound assessment of the lung shows the pleural line (red arrows) and hyperechoic regularly spaced horizontal repetitive lines (A lines) in control lungs (top panel). Irregular focal hyperechoic opacities distorting the pleural line are seen in infected subjects, characteristic of lung consolidation (white arrowheads). Edema and alveolar filling is evident from the hyperechoic vertical lines that obscure the normal A lines (highlighted with the red arrowheads). The B lines were consistent with the heterogeneous consolidation and lung injury seen on gross inspection (bottom panel; arrows). D, Sarkosyl extraction of plasma, heart and brain was performed and the resulting detergent insoluble fraction was probed for oligomeric tau using the T22 antibody. A representative western blot illustrates high T22-immunoreactive tau variants 48 hours following infection, with little immunoreactivity in an uninfected control. E, The normalized field excitatory post synaptic potential (fEPSP) slope was measured at the Schaffer collateral synapses in control and infected animals over a 60-minute time course (left-hand panel). A theta burst stimulation (TBS) was used to initiate long term potentiation (LTP). The dashed line represents the baseline values at time 0. Each group was comprised of 3 separate animals and LTP was recorded from 4-5 hippocampal slices per animal. The distribution of hippocampal slice recordings from different animals is plotted in the right-hand panel. Whereas LTP was not reduced 24 hours following infection ($p = $ ns vs control), it was decreased by ~50% 48 hours following infection ($P = .0003$ vs control and $P = .017$ vs 24 hours). Summary data were quantified from the last 5 minutes of the LTP response. Statistical differences were determined using one-way ANOVA with a Tukey's post hoc test

In addition, a non-specific IgG antibody was tested in infected animals. Amyloid and tau variants were then eluted from the antibody-bead complexes of the experimental and control groups with a high-salt solution and the salt was removed by centrifugation using a micro-concentrator and Hanks' balanced salt solution (HBSS). The antibody was denatured by boiling, releasing uncomplexed heat-stable amyloid and tau. Eluted cytotoxins were concentrated into a 600 μL volume of HBSS and 200 μL of the solution was introduced into the tracheas of three naïve, that is, uninfected, animals, so that each animal received the amyloid and tau from 1% of the plasma volume. Cardiac and pulmonary ultrasonography was performed and LTP measured 24 hours,

48 hours, and 1-month later. Left ventricular ejection fraction (Figure 2B) and cardiac output (data not shown) were not different between the antibody control and experimental groups. Amyloid and tau variants modestly injured the lung on gross inspection (Figure 2B,C) and tau variants isolated from the experimental group but not from the control groups were present in the plasma, heart, and brain (data not shown). LTP was suppressed at all three time-points (Figures 2E and S1B). Thus, pneumonia elicits a blood-borne cytotoxic amyloid and tau burden, and the amyloid and tau variants are sufficient to impair hippocampal information processing when they are introduced into the airways of uninfected animals.
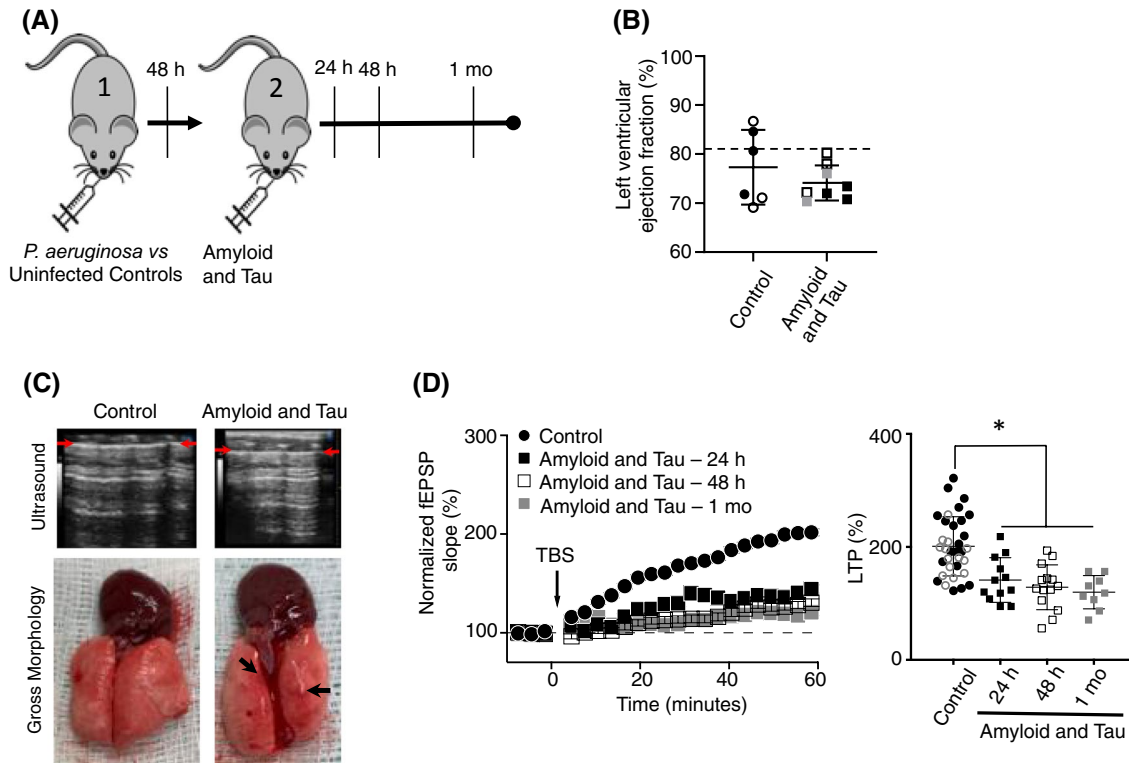
FIGURE 2 Amyloid and oligomeric tau variants present in the circulation post-infection cause end organ injury when introduced into the airways of naïve animals, that is, uninfected animals. A, Amyloid and tau species were captured from the plasma 48 hours after infection; the control and infected subjects are designated as "1". The amyloid and tau present in 1% of the plasma volume from these animals was introduced into the airway of a naïve subject, designated as "2", and peripheral organ function was tested at the indicated time points. B, Left ventricular ejection fraction was similar in control and experimental groups. Two groups comprised control subjects, including uninfected animals from which the A11 and T22 antibodies were used to capture circulating amyloid and tau (●) and infected animals from which an IgG antibody was used to non-selectively capture molecular species (○). Control animals were studied 48 hours after amyloid and tau introduction into the airway. Left ventricular ejection fractions were not different between these antibody controls and the uninfected control experiments that were reported in Figure 1 and are shown as a dashed line (*p* = ns using Student's t-test). Whereas amyloid and tau variants isolated from infected animals [24 hours (■), 48 hours (□), and 1 mo (■)] did not negatively impact left ventricular ejection fraction relative to antibody controls (*p* = ns), these values were significantly lower than the uninfected control animals (*P* = .007). Statistical differences were examined using one-way ANOVA with a Tukey's post hoc test and a Student's t-test. C, Representative ultrasound images of lungs from animals receiving amyloid and tau retrieved by A11 and T22 antibodies in both control and infected animals. Control and experimental animals demonstrate the usual pleural line (red arrows) and A lines (top panel). B lines were not commonly observed in these experiments. However, intermittent evidence for lung involvement was seen on gross morphology (arrows). D, The normalized fEPSP slope was measured at the Schaffer collateral synapses in animals receiving amyloid and tau isolated from control and infected subjects over a 60-minute time course (left-hand panel). A TBS was used to initiate LTP. The dashed line represents the baseline values at time 0. The control group included three animals inoculated with amyloid and tau collected by A11 and T22 antibodies in uninfected animals and three animals inoculated with molecular species collected using a non-specific IgG antibody in infected animals, each at the 48 hours time point. Controls were compared to an experimental group of animals that were inoculated with amyloid and tau collected by A11 and T22 antibodies from infected animals (n = 3). LTP was recorded from 4-5 hippocampal slices per animal. The distribution of hippocampal slice recordings from different animals is plotted in the right-hand panel. LTP was reduced at 24 hours (*P* =.001), 48 hours (*P* = .0001) and 1 mo (*P* = .0001) following amyloid and tau inoculation. Summary data were quantified from the last 5 minutes of the LTP response. Statistical differences were determined using one-way ANOVA with a Tukey's post hoc test

We next examined whether amyloid and tau can continue to be propagated among animals. To do this, A11- and T22-immunoreactive amyloid and tau, respectively, were collected from the circulation of amyloid- and tau-treated animals at the 1-month time point (Figure 3A). These cytotoxins were prepared as described above and inoculated into the tracheas of naïve animals. The amyloid and tau treatment elicited a modest time-dependent decrease in left ventricular ejection fraction (Figure 3B), did not impact cardiac output (data not shown), and caused lung injury (Figure 3C). Tau variants isolated from the experimental but not from the control groups were present in the
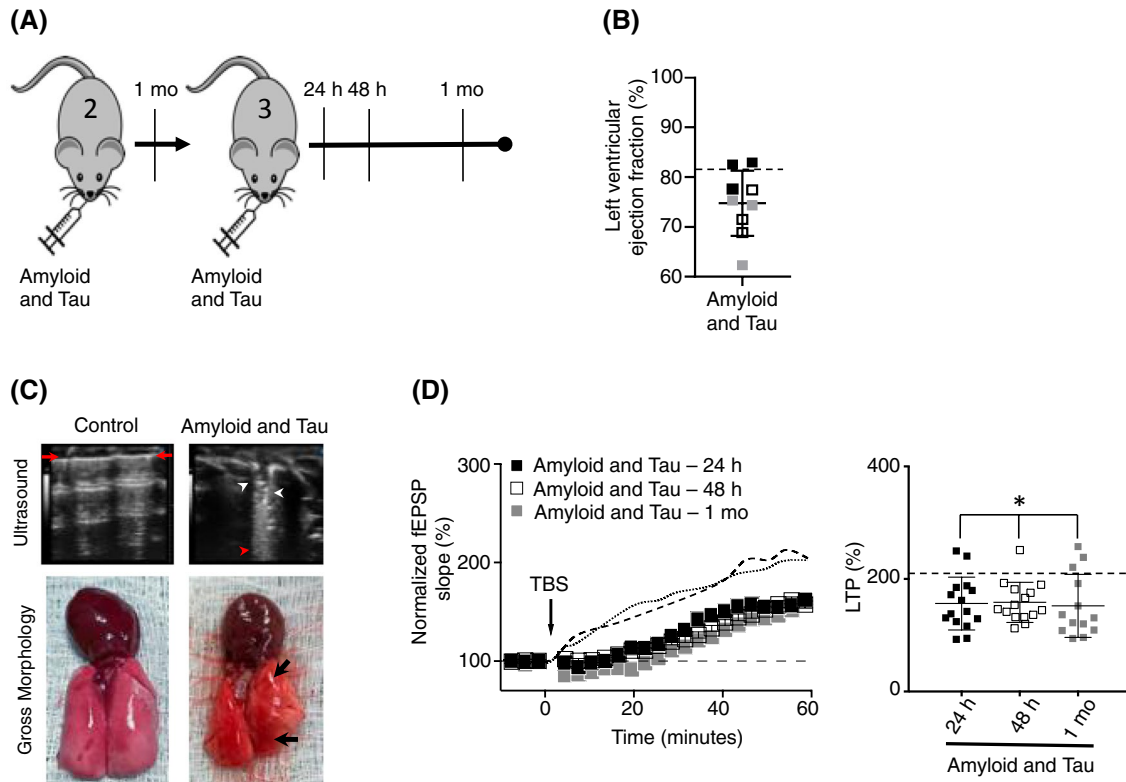
FIGURE 3 Amyloid and oligomeric tau variants present in the circulation after their intratracheal inoculation elicit a replicating injury in the absence of bacteria. A, Amyloid and oligomeric tau were captured from the plasma fraction of blood in the abdominal aorta 1 mo after amyloid and tau species were inoculated in the airways; this series of inoculations is designated as "2". The amyloid and tau present in 1% of the plasma volume were introduced into the airway of a naïve animal, designated as "3", and peripheral organ function was tested at the indicated time points. Note that control animals were not initially infected ("1—uninfected control" → "2—amyloid and tau inoculation") whereas the experimental group was initially infected with *P aeruginosa* ("1—*P aeruginosa* infection" → "2—amyloid and tau inoculation" → "3—amyloid and tau inoculation"). B, Because amyloid and tau did not impair organ function in control subjects, they were not collected from the 2nd control animals and inoculated into the 3rd animals in series; control values reported in Figure 2B are shown by a dashed line. Infection-derived amyloid and tau that were collected from the 2nd animals and introduced through the airway into the 3rd animals in series elicited a non-significant ($P = .10$) reduction in left ventricular ejection fraction when considering all time points together [24 hours (■), 48 hours (□), and 1 mo (■)], although the 48 hours ($P = .02$) and 1 mo ($P = .03$) time points were both reduced when compared to controls. Statistical differences were determined using one-way ANOVA with a Tukey's post hoc test and a Student's t-test. C, Representative lung ultrasound images are shown of subjects receiving intratracheal delivery of amyloid and tau collected from the plasma by A11 and T22 antibodies in control- and amyloid- and tau-treated animals. The control animal demonstrates the usual pleural line (red arrows) and A lines (top panel), whereas B lines were seen in the animal receiving amyloid and tau post-infection (highlighted with the red arrowheads). The B lines were consistent with the heterogeneous and minor lung injury (arrows) seen on gross inspection (bottom panel). D, The normalized fEPSP slope was measured at the Schaffer collateral synapses in animals receiving amyloid and tau from an infection series ("1—*P aeruginosa* infection" → "2—amyloid and tau inoculation" → "3—amyloid and tau inoculation") over a 60-minute time course (left-hand panel). A TBS was used to initiate LTP. The dashed line represents the baseline values at time 0. The control groups are representative of data plotted in Figure 1E (----) and Figure 2E (......). Controls were compared to an experimental group of animals that were inoculated with amyloid and tau collected by A11 and T22 antibodies from animals (n = 3) that received intratracheal delivery of amyloid and tau ("1—*P aeruginosa* infection" → "2—amyloid and tau inoculation" → "3—amyloid and tau inoculation"). LTP was recorded from 4-5 hippocampal slices per animal. The distribution of hippocampal slice recordings from different animals is plotted in the right-hand panel. LTP was reduced 24 hours ($P = .023$), 48 hours ($P = .034$) and 1 mo ($P = .017$) following amyloid and tau inoculation. Summary data were quantified from the last 5 minutes of the LTP response. Statistical differences were determined using one-way ANOVA with a Tukey's post hoc test

plasma, heart, and brain (data not shown). LTP was abolished within 24 hours post-inoculation and it remained low even throughout the 1-month time point (Figures 3E and S1C). Thus, infection-elicits a cytotoxic amyloid and tau burden in the circulation, and the introduction of these cytotoxins into the airways of uninfected animals is sufficient to chronically impair hippocampal information processing.

TABLE 1 Cytotoxic amyloid and tau are present in the ECMO oxygenators of pneumonia patients. (A) Patient demographics and clinical characteristics of the patients enrolled for this study. (B) Pathogenic etiology of pneumonia, defined as documented clinical suspicion from the treating physicians and presence of a positive culture from sputum, bronchoalveolar lavage, or viral respiratory panel within seven days of ECMO initiation, decannulation, or death

(A)

Demographics	No pneumonia n = 3	Pneumonia n = 8
Age (years)	63 (55-68)	51 (20-67)
Male	1 (33)	6 (75)
Body mass index (kg/m^2)	30 (27-37)	29 (22-40)
Race		
White	2 (67)	5 (63)
Asian	1 (33)	2 (25)
Unknown	0	1 (12)
Ethnicity		
Not Hispanic or Latino	3 (100)	7 (88)
Unknown	0 (0)	1 (12)
Medical history		
History of chronic lung disease	0	2 (25)
History of prior cardiac disease	1 (33)	2 (25)
SOFA score	10 (5-13)	9 (3-11)
APACHE II score	19 (10-26)	22 (14-27)
Pneumonia		
Bacterial	–	2 (25)
Viral	–	3 (37)
Polymicrobial	–	3 (37)
ECMO configuration and indication		
Veno-venous	1 (33)	3 (37)
ARDS	1 (100)	3 (100)
Veno-arterial	2 (67)	5 (63)
Post-cardiotomy	1 (34)	2 (25)
Myocardial infarction	0	2 (25)
Pulmonary embolism	1 (33)	0
ARDS	0	1 (13)
ECMO duration (days)	8 (4-16)	7 (5-12)
Hospital length of stay (days)	25 (16-31)	25 (9-175)
Survival to discharge	2 (67)	4 (50)

(B)

Patient	Pathogen
1	Methicillin-resistant *Staphylococcus aureus*

(Continues)

TABLE 1 (Continued)

(A)

Demographics	No pneumonia n = 3	Pneumonia n = 8
2	None	
3	Respiratory Syncytial Virus	
4	Influenza A (H1N1)	
5	Methicillin-sensitive *Staphylococcus aureus*, *Acinetobacter lwoffii*, *Klebsiella pneumoniae*	
6	*Klebsiella pneumoniae*	
7	None	
8	Adenovirus	
9	Rhinovirus/Enterovirus, Methicillin-resistant *Staphylococcus aureus*	
10	None	
11	*Morganella morganii*, *Enterobacter cloacae*	

Note: Data represented as n (%) or median (range).

Abbreviations: APACHE II, acute physiology and chronic health evaluation II (calculated within 24 hours of cannulation); ARDS, acute respiratory distress syndrome; ECMO, extracorporeal membrane oxygenation; SOFA, sequential organ failure assessment (calculated within 24 hours of cannulation).

3.2 | Tau variants are present in ECMO oxygenators of pneumonia patients

We next determined whether critically ill patients with pneumonia possess cytotoxic amyloid and tau variants in the circulation, and further, whether the oligomeric tau tracks with clinical outcomes. Oxygenators from 11 patients supported with VV or VA ECMO were studied. Pneumonia was defined retrospectively by a study investigator (AA) blinded to the cytotoxicity studies, as clinical suspicion documented by the treating clinicians with a confirmed culture (sputum, bronchoalveolar lavage [BAL] or viral respiratory panel) within seven days of initiating ECMO or until either decannulation or death. Clinical care was not altered for the purposes of this study. The median age of enrolled patients was 55 years (range 20-68) (Table 1). Four patients (36%) had respiratory failure and were on VV-ECMO and seven (64%) patients required VA-ECMO. The median duration of ECMO was 8 ± 3.4 days. Eight patients (73%) met the criteria for pneumonia (Table 1). The Sequential Organ Failure Assessment and the Acute Physiology and Chronic Health Evaluation II scores were not different among infected and uninfected patients. Six (55%) patients survived to
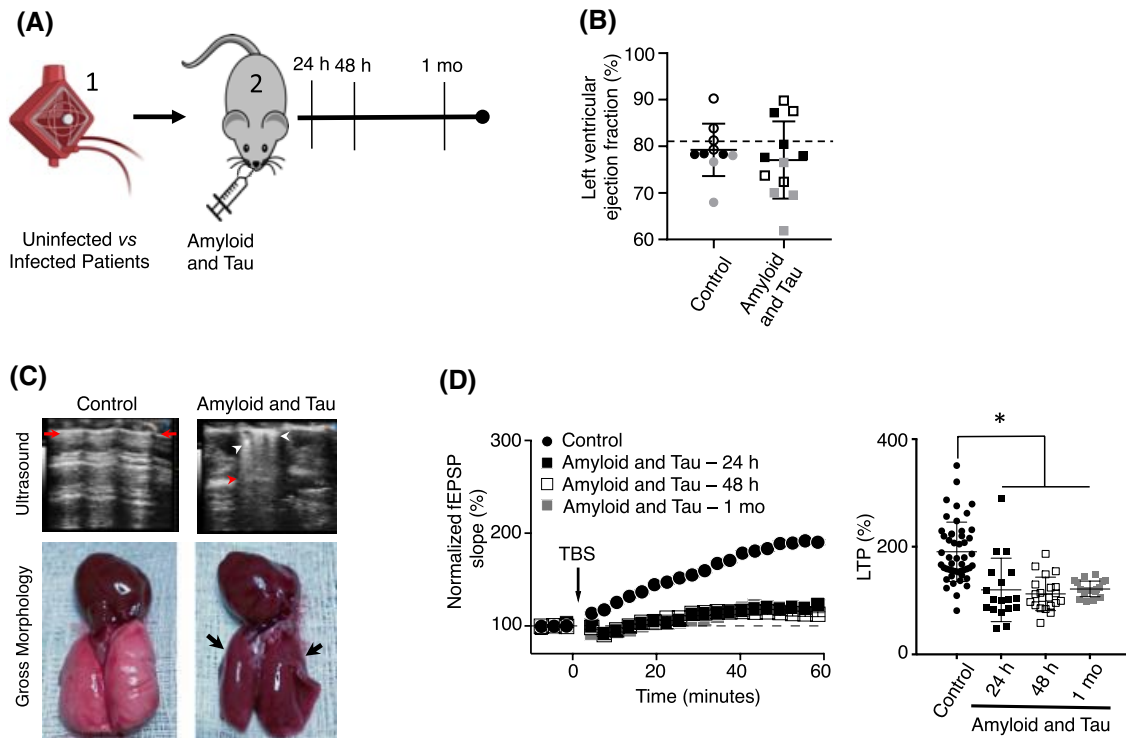
FIGURE 4 Amyloid and tau in ECMO oxygenator effluent of pneumonia patients are cytotoxic. A, Amyloid and tau captured from ~0.7% of the membrane oxygenator effluents (designated "1") using A11 and T22 antibodies were introduced into the airway of previously uninfected subjects (designated "2"). Controls included amyloid and tau collected from the membrane oxygenator effluent of patients 2, 7, and 10, none of whom harbored infection during extracorporeal support. Experimental samples were obtained from patients 1, 4, 9, and 11, all of whom had ongoing pneumonia at the time of ECMO oxygenator decannulation (see also Table S1). B, Amyloid and tau collected from the membrane oxygenator effluent of uninfected patients had no effect, whereas those isolated from the membrane oxygenator effluent of infected patients led to a time-dependent decrease in left ventricular ejection fraction, where 1 mo values (■) were lower than those at both 24 hours (■; $P = .02$) and 48 hours (□; $P = .01$). Statistical differences were determined using Student's t-test and one-way ANOVA with a Tukey's post hoc test. C, Representative lung ultrasound images are shown. The control animal demonstrates the usual pleural line (red arrows) and A lines (top panel). Lung consolidation (white arrowheads) with B lines characteristic of edema (highlighted with the red arrowheads) is shown. The B lines were consistent with the lung injury (arrows) seen on gross inspection (bottom panel). D, The normalized fEPSP slope was measured at the Schaffer collateral synapses in animals receiving amyloid and tau from the membrane oxygenator effluent of uninfected and infected subjects over a 60-minute time course (left-hand panel). A TBS was used to initiate LTP. The dashed line represents the baseline values at time 0. Whereas LTP was normal in control subjects, it was significantly reduced at all time points in the experimental groups (24 hours, $P = .0001$; 48 hours, $P = .0001$; and, 1 mo, $P = .0001$). LTP was recorded from 4-5 hippocampal slices per animal. The distribution of hippocampal slice recordings from different animals is plotted in the right-hand panel. Summary data were quantified from the last 5 minutes of the LTP response. Statistical differences were determined using one-way ANOVA with a Tukey's post hoc test

discharge. The clinical course of the 11 patients is summarized in Table S1.

De-identified oxygenators (ie, laboratory staff were blinded to clinical details) were flushed with 480 mL of HBSS containing calcium and magnesium within 24 hours of decannulation; residual blood within the oxygenator together with the HBSS was considered to be membrane oxygenator effluent. The membrane oxygenator effluent was centrifuged, separated into aliquots, and incubated on confluent monolayers of pulmonary microvascular endothelial cells for 24 hours. Effluent cytotoxicity was assessed by quantifying inter-endothelial cell gap formation and LDH release. Endothelial gap formation (Figure S2A,B) and cytotoxicity was only seen in patients with pneumonia. Effluent from patients without pneumonia (patients 2, 7, and 10) was non-cytotoxic and elicited no-to-minor increase in LDH.

To assess whether oligomeric tau was present in membrane oxygenator effluent, a T22-based ELISA was developed. T22 immunoreactivity of 1 mL of the membrane oxygenator effluent was compared to results obtained from an in vitro model of infection in which endothelial cell gap formation is due to cytotoxic amyloid and tau variants.[19,20] Cells were exposed to *P aeruginosa* (PA103*exoUexoT::Tc* pUCP*exoY*; MOI 20:1). Infection caused progressive

endothelial gap formation over 4-6 hours and release of cytotoxic amyloid and tau. Supernatant was then applied to cells in the absence of bacteria. Supernatant caused severe cytotoxicity (Figure S2B), an effect that is largely abolished by supernatant neutralization with the T22 antibody.[19,20] Undiluted and serially diluted supernatant was tested for T22 immunoreactivity and this result was directly compared to the results obtained with membrane oxygenator effluents. T22 immunoreactivity was not different between the endothelial supernatant and the non-cytotoxic membrane oxygenator effluent (effluent

that did not cause endothelial gap formation), however, it increased 2.5-fold in cytotoxic membrane oxygenator effluent (Figure S2C). Effluent from the oxygenators of patients with pneumonia had high concentrations of T22 immunoreactive amyloids. Samples were also boiled and their T22 immunoreactive signal re-assessed.[19] Boiling the oxygenator membrane effluent reduced the T22 immunoreactive signal in 7 of the 11 samples (Figure S2D). Four samples demonstrated increased T22 immunoreactivity after boiling—these four samples corresponded to the four patients that died (Figure S2D and Table S1). Thus, boiling
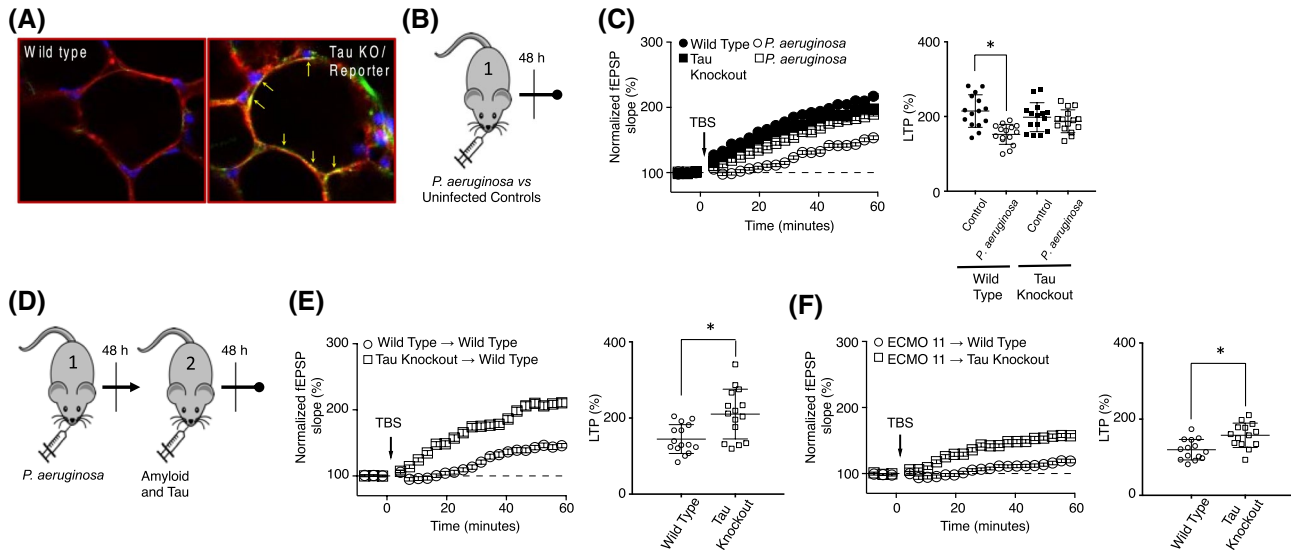

FIGURE 5 Infection-induced amyloid and tau cytotoxicity requires tau. A, Lung capillaries express tau. Fluorescence of wild type (left panel) and tau knockout (KO; right panel) mice were tested. Cell nuclei were stained with NucBlue and the endothelium was labeled with tomato lectin (*Lycopersicon esculentum*) through the circulation. The circulation and airways of wild type and knockout mice were then filled with gelatin and agarose, respectively. The B6.129S4(Cg)-*Mapt^{tm1(EGFP)/Klt}*/J mouse harbors a tau knockout with an EGFP insertion in exon 1 of the tau locus so that tau-expressing cells can be visualized. Three hundred micron-thick lung sections were cut, and the alveolus was imaged by high resolution confocal microscopy. Lung capillaries exhibited green, that is, EGFP, and red, that is, tomato lectin, fluorescence, indicating that they express endothelial tau under basal conditions. Yellow arrows show areas of overlap between the tau reporter and tomato lectin labeling of capillary endothelium. B, *P aeruginosa* was introduced directly into the airway of wild type and tau knockout mice and long-term potentiation was measured 48 hours later. C, The normalized fEPSP slope was measured at the Schaffer collateral synapses in control and infected animals over a 60-minute time course (left-hand panel). A TBS was used to initiate LTP. The dashed line represents the baseline values at time 0. Each group was comprised of 3 separate animals and LTP was recorded from 4-5 hippocampal slices per animal. The distribution of hippocampal slice recordings from different animals is plotted in the right-hand panel. LTP was similar in uninfected wild type and tau knockout mice (p = ns). Whereas LTP was reduced following infection of wild type mice (P = .0001), it was not decreased following infection of tau knockout mice (p = ns). Summary data were quantified from the last 5 minutes of the LTP response. Statistical differences were determined using one-way ANOVA with a Tukey's post hoc test. D, Amyloid and tau were isolated from the plasma of wild type and tau knockout mice following infection, using the A11 and T22 antibodies. Amyloid and tau were then introduced into wild-type animals and long-term potentiation was measured 48 hours later. E, The normalized fEPSP slope was measured at the Schaffer collateral synapses in control and infected animals over a 60-minute time course (left-hand panel). A TBS was used to initiate LTP. The dashed line represents the baseline values at time 0. Each group was comprised of 3 separate animals and LTP was recorded from 4-5 hippocampal slices per animal. The distribution of hippocampal slice recordings from different animals is plotted in the right-hand panel. LTP was reduced in animals receiving amyloid and tau from wild type mice (P = .002), but it was not decreased following introduction of amyloid and tau from tau knockout mice (p = ns). Summary data were quantified from the last 5 minutes of the LTP response and statistical significance determined using a Student's t-test and a Mann–Whitney test. F, Amyloid and tau collected from ECMO patient 11 (*M morganii* pneumonia) were introduced into the tail vein of wild type and tau knockout mice. Forty-eight h later LTP was measured. Whereas the amyloid and tau inhibited LTP in wild type animals, LTP was preserved in tau knockout animals (n = 2 wild type and tau knockout animals analyzing 14 hippocampal brain slice recordings; P = .003 by Mann-Whitney test)

membrane oxygenator effluent samples altered the access of T22 to its immunoreactive epitope(s), revealing high concentrations of tau variants in the membrane oxygenator effluents of deceased patients.

We determined whether oligomeric tau present within membrane oxygenator effluents are sufficient to impair long-term potentiation in uninfected animals. A11- and T22-immunoreactive amyloid and tau variants, respectively, were collected from 10 mL of the membrane oxygenator effluents (~0.7% of the effluent), concentrated into a 200 μL volume, introduced into the airways of animals (Table 1 and Figure 4A), and end-organ function was evaluated 24 hours, 48 hours, and 1-month later. Left ventricular ejection fraction (Figure 4B) and cardiac output (data not shown) was within the normal range in both the control and experimental groups. Amyloid and tau isolated from the oxygenators of uninfected patients caused no remarkable lung injury, especially at the 1-month time point (Figures 4C and S3). In stark contrast, lung injury was seen in all animals receiving the amyloid and tau variants that were isolated from pneumonia-positive patients (Figure 4D). Summary data reveal that none of the uninfected patient samples impaired LTP, yet cytotoxic amyloid and tau isolated from patients who died, including patients 1, 4, 9, and 11, uniformly abolished LTP at all time points (Figure 4E). The individual LTP responses in animal subjects receiving amyloid and tau from both control and pneumonia patients is shown in Figures S4 and S5C. It is notable that amyloid and tau generated by both bacterial and viral pneumonias reduced LTP. However, the cytotoxins elicited by bacterial infections caused the most pronounced LTP suppression, whereas those generated during influenza A H1N1 infection most prominently inhibited LTP at the 48 hours and 1-month time points. Our findings indicate that cytotoxic amyloid and tau variants are present in the ECMO oxygenators of pneumonia patients, and they are sufficient to disrupt hippocampal information processing when introduced into uninfected animals.

3.3 | The impaired hippocampal information processing requires tau

This work supports the idea that pneumonia leads to the production of cytotoxic amyloid and tau variants that impair information processing in the hippocampus. To test the importance of tau in this process, we utilized a tau knockout mouse in which EGFP was introduced into the exon 1 locus as a reporter; tau-expressing cells therefore exhibit green fluorescence. NucBlue and Tomato lectin (*Lycopersicon esculentum*) were introduced through the circulation to visualize nuclei and endothelium, respectively. Figure 5A illustrates lung capillary endothelium constitutively expresses tau.

P aeruginosa (PA103*exoUexoT::Tc* pUCP*exoY*) was introduced into the airways of wild type and tau knockout mice. Forty-eight h following infection, cardiac ultrasonography revealed a hyperdynamic state in both wild type and knockout mice (data not shown). LTP was assessed as a primary endpoint (Figure 5B). Whereas the infection suppressed LTP in wild type animals, it did not reduce LTP in the tau knockout mice (Figures 5C and S5B). Amyloid and tau variants were isolated from the circulation of these infected mice and introduced into the airways of wild type animals (Figure 5D). Whereas the amyloid and tau generated by infection of wild type mice suppressed LTP, those generated by infection of tau knockout mice were without effect (Figures 5E and S5C). Therefore, tau is necessary for the infection-induced proteopathy that culminates in impaired learning and memory.
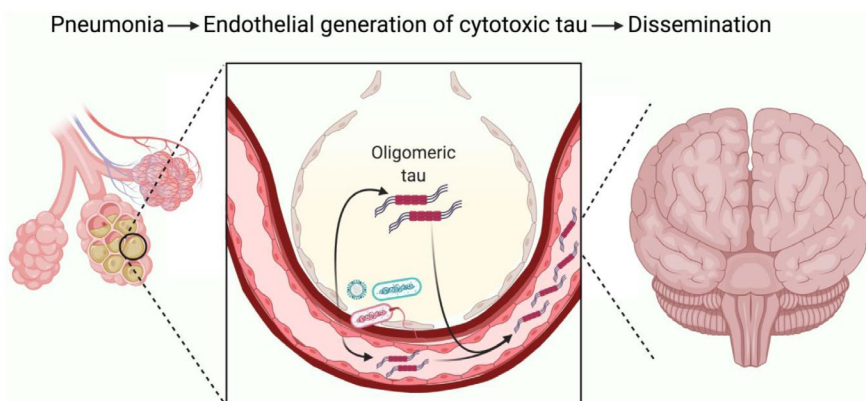

FIGURE 6 Pneumonia elicits the production of cytotoxic amyloid and tau within the lung. Lung infection (red and green rods represent bacteria and the green sphere represents a virus) promotes endothelial production of oligomeric tau. This oligomeric tau can be detected in the airways, circulation, cerebrospinal fluid, and the brain. Pneumonia leads to impairment of long-term potentiation in the hippocampus, and this effect requires tau

We examined whether tau was also necessary for amyloid and tau isolated from membrane oxygenator effluents to impair long term potentiation. Amyloid and tau variants isolated from patient 11 (*M morganii* infection) were introduced into the circulation through the tail vein of wild type and tau knockout mice. Forty-eight h later, LTP was assessed. Introduction of the amyloid and tau species into the circulation was sufficient to decrease LTP in wild type mice (Figure 5F). LTP in knockout mice was lower than it was in control animals ($P = .02$, one-way ANOVA with Tukey's post hoc test) yet preserved when compared to the wild-type mouse (Figure 5F). These data support the idea that tau is an essential component of the infection-induced cytotoxin that impairs hippocampal information processing.

4 | DISCUSSION

Here, we report that pneumonia initiates the production of cytotoxic amyloid and tau by lung endothelium and perhaps other cell types in vivo. These cytotoxins disseminate through the circulation, access the brain, and either directly or indirectly impair hippocampal long-term potentiation. Direct introduction of the infection-derived, blood-borne amyloid and tau variants into either the airways or the blood of otherwise uninfected animals culminates in impaired hippocampal long-term potentiation. This debilitating effect on hippocampal information processing requires tau.

Evidence in support of this infectious tauopathy hypothesis (Figure 6), and the role of the lung endothelium in the production of cytotoxic tau variants, include the following. First, tau is constitutively expressed in lung capillary endothelium, at the alveolar-capillary membrane (Figure 5A), and it is expressed by lung endothelium in vitro.[24,30,31] Second, bacterial and viral pneumonias lead to accumulation of oligomeric tau in the airways,[19,20] circulation (Figure 1D), heart (Figure 1D), cerebrospinal fluid,[20,21] and brain tissue[21,22]; this interpretation is based upon immunoreactivity with tau-reactive antibodies, including T22, TNT1, and Tau5. The T22-immunoreactive species are detected in sarkosyl-insoluble detergent samples, consistent with cytotoxic tau variants. Third, the appearance of sarkosyl-insoluble tau in the cerebrospinal fluid and hippocampus following infection corresponds with impaired LTP and loss of dendritic spine density.[21,22] Moreover, cerebrospinal fluid isolated from mechanically ventilated patients with ongoing pneumonia, but not from mechanically ventilated patients without infection, impairs LTP within the rodent hippocampus.[20] This inhibition of LTP is abolished when amyloid and tau are removed from the cerebrospinal fluid using neutralizing

antibodies, including A11 and T22 antibodies, and it is rescued when tau variants are eluted from anti-tau neutralizing antibodies and applied directly to the hippocampus[20]; this acute tau-dependent inhibition of LTP cannot be attributed to cytokines, hypoxia, hypoperfusion, or any anesthetic, analgesic, or sedative medication. Fourth, the direct application of oligomeric tau isolated from the blood of rodents and humans with ongoing infection (Figures 2-5), and from supernatants of endothelial cells exposed to pneumonia-causing pathogens,[21,22] into either the airway or the circulation is sufficient to impair brain function. Fifth, hippocampal LTP is preserved following pneumonia and exposure to cytotoxic amyloid and tau in the tau knockout mouse (Figure 5). Tau is an essential contributor to infectious proteopathy.

The transmission of cytotoxic misfolded proteins from one subject to another is a characteristic of prion disease(s). We did not test whether animals with pneumonia are capable of transferring cytotoxic amyloid and tau to uninfected animals during the course of their illness. However, we found that direct introduction of cytotoxic amyloid and tau isolated from mice, rats, and humans into either the airways or blood of uninfected rodents culminates in impaired hippocampal information processing. The amyloid and tau that is produced during lung infection is neurotropic, similar to other proteopathies that include Kuru, Bovine Spongiform Encephalopathy, and Creutzfeldt-Jakob Disease, among others.[32,33]

The molecular basis of the cytotoxic amyloid and tau isolated from different species (ie, mice, rats, and humans) and from diverse causes of pneumonia (ie, bacterial and viral) is not presently resolved. However, the common function(s) of these cytotoxins is/are consistent with a common molecular basis. It is notable that in each of these cases, the amyloid and tau isolated from a small plasma volume was sufficient to impair brain function. The extent to which bronchoalveolar lavage fluid, blood and cerebrospinal fluid from infected patients represents a transmissible threat to health care providers and others has yet to be established.

The majority (~90%) of prion diseases is sporadic in nature. This is also the case for tauopathies, which include Alzheimer's disease, progressive supranuclear palsy, Pick's disease, and corticobasal syndrome.[34,35] Although the mechanism(s) responsible for the initial tau misfolding in these sporadic cases is/are unknown, once misfolded into oligomer or aggregate forms, the misfolded tau is capable of seeding new oligomers and aggregates important for disease progression.[36-39] Moreover, the introduction of misfolded tau from the brains of these subjects into otherwise normal animals results in a progressive tauopathy.[39-45] Significant heterogeneity in pathogenic tau strains has been reported, especially regarding the extent of tau phosphorylation and

Infectious tauopathy hypothesis

1. Oligomeric tau transport or cerebrovascular barrier dysruption

2. Proteopathic tau seeding

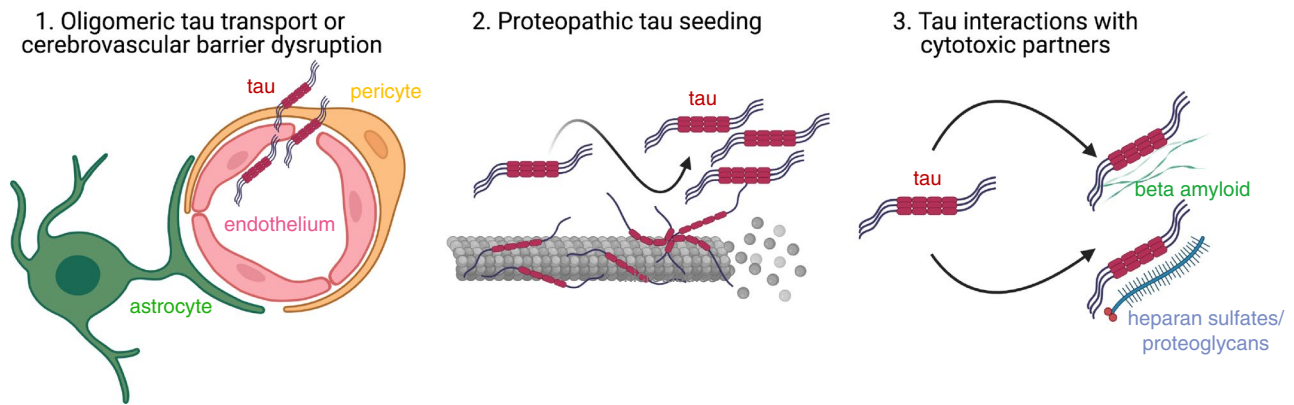### 3. Tau interactions with cytotoxic partners

FIGURE 7 Pneumonia-induced oligomeric tau (red) accesses the brain where it impairs LTP in the hippocampus. Oligomeric tau is generated by endothelium within the lung and disseminates through the circulation. Important questions remain unanswered regarding whether oligomeric tau: (1) is transported across the blood–brain barrier, increases blood–brain barrier permeability, or both (astrocyte is green, pericyte is orange, endothelium is light red); (2) induces amplification by proteopathic seeding in the circulation or the brain (microtubule is gray); and, (3) interacts with other potentially injurious biomolecules, like some forms of heparan sulfates/proteoglycans (bottom, blue) and beta amyloid (top, green), to promote neuroinflammation and cytotoxicity

its propensity to seed or spread throughout the brain.[39,42] Our findings indicate that pneumonia is the cause of a different, but related, "sporadic" tauopathy endotype, and it may contribute to delirium and long-term cognitive dysfunction associated with critical illness.[16,18,46,47]

We describe two phases of this pneumonia-induced tauopathy endotype. The short-term LTP impairment is likely due to reduced postsynaptic ion channel activation, permeation, recruitment, and spine remodeling.[48,49] This short-term impairment in postsynaptic signaling transitions into a long-term loss of dendritic spines.[20,22] Future studies are warranted to determine whether the pneumonia-initiated tauopathy is sufficient to reduce postsynaptic spine density as a progression toward dementia, as infections may contribute to, or even be a cause of, irreversible disease like Alzheimer's disease and post-intensive care unit dementia.[16,18,46,47]

Cytotoxic tau was present in the circulation of patients on ECMO who had evidence of pneumonia, either as a primary cause of respiratory failure or who developed it during their extracorporeal course. Critically ill patients who fail standard medical therapy may receive pulmonary or cardiac support from extracorporeal membrane oxygenation (ECMO). The ECMO to Rescue Lung Injury in Severe Acute Respiratory Distress Syndrome (EOLIA) trial showed a trend towards improved survival and a significant reduction in the need for vasopressors, dialysis and proning in ECMO-enrolled subjects with severe acute respiratory distress syndrome.[50] Follow-up meta-analysis and Bayesian analyses supported the interpretation that ECMO offers benefit for severely ill acute respiratory distress syndrome patients.[51,52] Future

studies will be required to assess whether the oxygenators capture amyloid and tau variants from the circulation and confer some benefit, and whether circulating tau represents a prognostic biomarker for end organ dysfunction.

We measured cardiac function during infection and cytotoxic amyloid and tau exposure to assess whether decreased cardiac output could contribute to impaired brain function, since cardiac dysfunction is common in pneumonia patients.[53,54] We observed increased left ventricular ejection fraction and cardiac output in response to acute infection, consistent with a hyperdynamic state during sepsis. We observed modest decrements in left ventricular ejection fraction during the latter time points of amyloid and tau exposure, yet cardiac output was not reduced. Decreased cardiac output cannot explain impaired hippocampal long-term potentiation.

There are limitations to our study. We do not currently know how the circulating amyloid and tau species access the brain and function within the cerebrospinal fluid and the brain; this is a focus of active investigation. We consider three important issues that impact amyloid and tau translocation from the circulation to the brain, and the cytotoxicity of amyloids and tau once they are in the brain (Figure 7). First, circulating amyloid and tau species may be transported across the blood–brain barrier dependent upon the low-density lipoprotein receptor-related protein 1.[55] Alternatively, they may disrupt the endothelium and adjoining cells lining either the blood–brain barrier or the choroid plexus, leading to increased permeability.[19,20,26] Irrespective of the mechanism, cytotoxic amyloid and tau appears within the brain shortly after the onset of pneumonia.

Second, either in the circulation or once they are in the brain, amyloid and tau variants may initiate a feed-forward response, promoting the nucleation of monomeric tau and/or other amyloid species into cytotoxic oligomers.[37] In our study, the introduction of cytotoxic amyloid and tau into the circulation abolished LTP in wild-type animals, whereas LTP was preserved, albeit below control values, in tau knockout animals. These data indicate that circulating cytotoxic amyloid and tau variants access the brain from the circulation, but also, that there may be amplification of cytotoxic activity that requires endogenously expressed tau.[37,56] Future studies will be required to address mechanisms of cytotoxic tau propagation during the natural course of infection. Although proteopathic tau seeding may represent an important mechanism of insidious brain injury in the aftermath of an infection, it is unlikely that oligomeric tau acts alone to elicit dysfunctional neuronal signaling. The oligomeric tau may promote neuroinflammation that contributes to impaired signaling and neuronal structural remodeling. The extent to which oligomeric tau acts alone or together with other mechanisms of neuroinflammation will need to be addressed.

Third, our studies provide mechanistic insight into the molecular makeup of the infection-induced cytotoxic amyloid and tau variants: tau is an essential contributor. However, oligomeric tau may interact with other molecular species, like glycosaminoglycans[57] and beta amyloid,[19,20,26] that are generated during infection. Future studies will be required to determine how these intermolecular interactions influence cytotoxicity during the natural course of infection.

In conclusion, our work unequivocally indicates that pneumonia elicits lung endothelial amyloid and tau variants that disseminate through the circulation and cause impaired hippocampal information processing. The cytotoxicity requires tau. These cytotoxic tau variants represent a new class of infection-dependent biomolecules that we incriminate in the tissue injury seen in patients recovering from pneumonia,[58,59] critical illness dementia,[16,60,61] and perhaps the so-called COVID-19 long-haulers.[62-64]

CONFLICT OF INTEREST
The authors have no conflicts of interest.

AUTHOR CONTRIBUTIONS
T. Stevens, R. Balczon, M.T. Lin, and C.E. Ventetuolo conceived of and guided the research; C. Zhou, J.Y. Lee, and T. Stevens performed ultrasound experiments and conducted the surgeries; M.T. Lin performed brain electrophysiological recordings; R. Balczon isolated amyloids from plasma and tissues and performed Western blots; S.B. Voth maintained bacterial stocks; P. Renema, S.B. Voth, and C.-S. Choi prepared bacteria for inoculations and A. Koloteva performed intratracheal delivery of bacteria and amyloids; C.M. Francis quantified and analyzed endothelial cell gap formation; A. Abbasi, C.E. Ventetuolo, B.M. Wagener, and J.-F. Pittet provided clinical assessment of pneumonia and guided the clinical research; N.R. Sodha placed ECMO cannulas, supervised the care of patients enrolled in this study and oversaw decannulation; A. Abbasi was responsible for communicating with the Stevens lab and providing de-identified ECMO filters for analysis; A. Abbasi and J. Bell maintained data records.

ORCID
Ron Balczon https://orcid.org/0000-0001-8263-7221
Mike T. Lin https://orcid.org/0000-0002-9806-8198
Ji Young Lee https://orcid.org/0000-0002-8005-2446
Adeel Abbasi https://orcid.org/0000-0001-7887-243X
Phoibe Renema https://orcid.org/0000-0003-0230-7068
Sarah B. Voth https://orcid.org/0000-0003-3796-7154
C. Michael Francis https://orcid.org/0000-0001-6001-2618
Jean-Francois Pittet https://orcid.org/0000-0002-2196-9289
Brant M. Wagener https://orcid.org/0000-0001-7889-1526
Corey E. Ventetuolo https://orcid.org/0000-0002-4223-4775
Troy Stevens https://orcid.org/0000-0001-9689-929X

REFERENCES
1. Naghavi M, Abajobir AA, Abbafati C, et al. Global, regional, and national age-sex specific mortality for 264 causes of death, 1980–2016: a systematic analysis for the Global Burden of Disease Study 2016. *Lancet*. 2017;390:1151-1210.
2. Troeger C, Blacker B, Khalil IA, et al. Estimates of the global, regional, and national morbidity, mortality, and aetiologies of

lower respiratory infections in 195 countries, 1990–2016: a systematic analysis for the Global Burden of Disease Study 2016. *Lancet Infect Dis*. 2018;18:1191-1210.

3. Ackermann M, Verleden SE, Kuehnel M, et al. Pulmonary vascular endothelialitis, thrombosis, and angiogenesis in COVID-19. *N Engl J Med*. 2020;383:120-128.

4. Chen N, Zhou M, Dong X, et al. Epidemiological and clinical characteristics of 99 cases of 2019 novel coronavirus pneumonia in Wuhan, China: a descriptive study. *Lancet*. 2020;395:507-513.

5. Zhu NA, Zhang D, Wang W, et al. A novel coronavirus from patients with pneumonia in China, 2019. *N Engl J Med*. 2020;382:727-733.

6. Hermans G, Van Aerde N, Meersseman P, et al. Five-year mortality and morbidity impact of prolonged versus brief ICU stay: a propensity score matched cohort study. *Thorax*. 2019;74: 1037-1045.

7. Ou S-M, Chu H, Chao P-W, et al. Long-term mortality and major adverse cardiovascular events in sepsis survivors. A nationwide population-based study. *Am J Respir Crit Care Med*. 2016;194:209-217.

8. Yende S, Linde-Zwirble W, Mayr F, Weissfeld LA, Reis S, Angus DC. Risk of cardiovascular events in survivors of severe sepsis. *Am J Respir Crit Care Med*. 2014;189:1065-1074.

9. Brummel NE, Bell SP, Girard TD, et al. Frailty and subsequent disability and mortality among patients with critical illness. *Am J Respir Crit Care Med*. 2017;196:64-72.

10. Brummel NE, Jackson JC, Pandharipande PP, et al. Delirium in the ICU and subsequent long-term disability among survivors of mechanical ventilation. *Crit Care Med*. 2014;42:369-377.

11. Fan E, Dowdy DW, Colantuoni E, et al. Physical complications in acute lung injury survivors: a two-year longitudinal prospective study. *Crit Care Med*. 2014;42:849-859.

12. Ferrante LE, Murphy TE, Leo-Summers LS, Gahbauer EA, Pisani MA, Gill TM. The Combined effects of frailty and cognitive impairment on post-ICU disability among older ICU survivors. *Am J Respir Crit Care Med*. 2019;200:107-110.

13. Ferrante LE, Pisani MA, Murphy TE, Gahbauer EA, Leo-Summers LS, Gill TM. Functional trajectories among older persons before and after critical illness. *JAMA Intern Med*. 2015;175:523-529.

14. Girard TD, Jackson JC, Pandharipande PP, et al. Delirium as a predictor of long-term cognitive impairment in survivors of critical illness. *Crit Care Med*. 2010;38:1513-1520.

15. Hopkins RO, Weaver LK, Collingridge D, Parkinson RB, Chan KJ, Orme JF Jr. Two-year cognitive, emotional, and quality-of-life outcomes in acute respiratory distress syndrome. *Am J Respir Crit Care Med*. 2005;171:340-347.

16. Iwashyna TJ, Ely EW, Smith DM, Langa KM. Long-term cognitive impairment and functional disability among survivors of severe sepsis. *JAMA*. 2010;304:1787-1794.

17. Jackson JC, Pandharipande PP, Girard TD, et al. Depression, post-traumatic stress disorder, and functional disability in survivors of critical illness in the BRAIN-ICU study: a longitudinal cohort study. *Lancet Respir Med*. 2014;2:369-379.

18. Pandharipande PP, Girard TD, Jackson JC, et al. Long-term cognitive impairment after critical illness. *N Engl J Med*. 2013;369:1306-1316.

19. Balczon R, Morrow KA, Zhou C, et al. *Pseudomonas aeruginosa* infection liberates transmissible, cytotoxic prion amyloids. *FASEB J*. 2017;31:2785-2796.

20. Lin MT, Balczon R, Pittet J-F, et al. Nosocomial pneumonia elicits an endothelial proteinopathy: evidence for a source of neurotoxic amyloids in critically ill patients. *Am J Respir Crit Care Med*. 2018;198:1575-1578.

21. Balczon R, Pittet J-F, Wagener BM, et al. Infection-induced endothelial amyloids impair memory. *FASEB J*. 2019;33:10300-10314.

22. Scott AM, Jager AC, Gwin M, et al. Pneumonia-induced endothelial amyloids reduce dendritic spine density in brain neurons. *Sci Rep*. 2020;10:9327

23. Alexeyev M, Geurts AM, Annamdevula NS, et al. Development of an endothelial cell-restricted transgenic reporter rat: a resource for physiological studies of vascular biology. *Am J Physiol Heart Circ Physiol*. 2020;319:H349-H358.

24. Ochoa CD, Alexeyev M, Pastukh V, Balczon R, Stevens T *Pseudomonas aeruginosa* exotoxin Y is a promiscuous cyclase that increases endothelial tau phosphorylation and permeability. *J Biol Chem*. 2012;287:25407-25418.

25. Sayner SL, Frank DW, King J, Chen H, VandeWaa J, Stevens T. Paradoxical cAMP-induced lung endothelial hyperpermeability revealed by *Pseudomonas aeruginosa* ExoY. *Circ Res*. 2004;95:196-203.

26. Voth S, Gwin M, Francis CM, et al. Virulent *Pseudomonas aeruginosa* infection converts antimicrobial amyloids into cytotoxic prions. *FASEB J*. 2020;34:9156-9179.

27. Lee JY, Fagan KA, Zhou C, Batten L, Cohen MV, Stevens T. Biventricular diastolic dysfunction, thrombocytopenia, and red blood cell macrocytosis in experimental pulmonary arterial hypertension. *Pulm Circ*. 2020;10:2045894020908787.

28. Kanaan NM, Cox K, Alvarez VE, Stein TD, Poncil S, McKee AC. Characterization of early pathological tau conformations and phosphorylation in chronic traumatic encephalopathy. *J Neuropathol Exp Neurol*. 2016;75:19-34.

29. American Thoracic S. and Infectious Diseases Society of, A. Guidelines for the management of adults with hospital-acquired, ventilator-associated, and healthcare-associated pneumonia. *Am J Respir Crit Care Med*. 2005;171:388-416.

30. Balczon R, Prasain N, Ochoa C, et al. *Pseudomonas aeruginosa* exotoxin Y-mediated tau hyperphosphorylation impairs microtubule assembly in pulmonary microvascular endothelial cells. *PLoS ONE*. 2013;8:e74343.

31. Morrow KA, Ochoa CD, Balczon R, et al. *Pseudomonas aeruginosa* exoenzymes U and Y induce a transmissible endothelial proteinopathy. *Am J Physiol Lung Cell Mol Physiol*. 2016;310:L337-353.

32. Prusiner S. Shattuck lecture—neurodegenerative diseases and prions. *N Engl J Med*. 2001;344:1516-1526.

33. Scheckel C, Aguzzi A. Prions, prionoids and protein misfolding disorders. *Nat Rev*. 2018;19:405-418.

34. Stanford PM, Brooks WS, Teber ET, et al. Frequency of tau mutations in familial and sporadic frontotemporal dementia and other tauopathies. *J Neurol*. 2004;251:1098-1104.

35. Lee V-Y, Goedert M, Trojanowski J. Neurodegenerative tauopathies. *Annu Rev Neurosci*. 2001;24:1121-1159.

36. Bell BJ, Malvankar MM, Tallon C, Slusher BS. Sowing the seeds of discovery: tau-propagation models of Alzheimer's disease. *ACS Chem Neurosci*. 2020;11:3499-3509.

37. Holmes BB, Furman JL, Mahan TE, et al. Proteopathic tau seeding predicts tauopathy in vivo. *Proc Natl Acad Sci U S A*. 2014;111:E4376-E4385.

38. Kaufman SK, Sanders DW, Thomas TL, et al. Tau prion strains dictate patterns of cell pathology, progression rate, and regional vulnerability *in vivo*. *Neuron*. 2016;92:796-812.

39. Sanders D, Kaufman S, DeVos S, et al. Distinct tau prion strains propagate in cells and mice and define different tauopathies. *Neuron*. 2014;82:1271-1288.

40. Clavaguera F, Akatsu H, Fraser G, et al. Brain homogenates from human tauopathies induce tau inclusions in mouse brain. *Proc Natl Acad Sci*. 2013;110:9535-9540.

41. Clavaguera F, Bolmont T, Crowther RA, et al. Transmission and spreading of tauopathy in transgenic mouse brain. *Nat Cell Biol*. 2009;11:909-913.

42. Dujardin S, Commins C, Lathuiliere A, et al. Tau molecular diversity contributes to clinical heterogeneity in Alzheimer's disease. *Nat Med*. 2020;26:1256-1263.

43. He Z, McBride JD, Xu H, et al. Transmission of tauopathy strains is independent of their isoform composition. *Nat Commun*. 2020;11:7.

44. Lasagna-Reeves CA, Castillo-Carranza DL, Sengupta U, et al. Alzheimer brain-derived tau oligomers propagate pathology from endogenous tau. *Sci Rep*. 2012;2:700.

45. Takeda S, Wegmann S, Cho H, et al. Neuronal uptake and propagation of a rare phosphorylated high-molecular-weight tau derived from Alzheimer's disease brain. *Nat Commun*. 2015;6:8490.

46. Mikkelsen ME, Christie JD, Lanken PN, et al. The adult respiratory distress syndrome cognitive outcomes study: long-term neuropsychological function in survivors of acute lung injury. *Am J Respir Crit Care Med*. 2012;185:1307-1315.

47. Shah FA, Pike F, Alvarez K, et al. Bidirectional relationship between cognitive function and pneumonia. *Am J Respir Crit Care Med*. 2013;188:586-592.

48. Collingridge G, Isaac J, Wang Y. Receptor trafficking and synaptic plasticity. *Nat Rev Neurosci*. 2004;5:952-962.

49. Shi S, Hayashi Y, Petralia R, et al. Rapid spine delivery and redistribution of AMPA receptors after synaptic NMDA receptor activation. *Science*. 1999;284:1811-1816.

50. Combes A, Hajage D, Capellier G, et al. Extracorporeal membrane oxygenation for severe acute respiratory distress syndrome. *N Engl J Med*. 2018;378:1965-1975.

51. Goligher EC, Tomlinson G, Hajage D, et al. Extracorporeal membrane oxygenation for severe acute respiratory distress syndrome and posterior probability of mortality benefit in a post hoc Bayesian analysis of a randomized clinical trial. *JAMA*. 2018;320:2251-2259.

52. Munshi L, Walkey A, Goligher E, Pham T, Uleryk EM, Fan E. Venovenous extracorporeal membrane oxygenation for acute respiratory distress syndrome: a systematic review and meta-analysis. *Lancet Respir Med*. 2019;7:163-172.

53. Corrales-Medina VF, Alvarez KN, Weissfeld LA, et al. Association between hospitalization for pneumonia and subsequent risk of cardiovascular disease. *JAMA*. 2015;313:264-274.

54. Corrales-Medina V, Musher D, Shachkina S, Chirinos J. Acute pneumonia and the cardiovascular system. *Lancet*. 2013;381:496-505.

55. Rauch JN, Luna G, Guzman E, et al. LRP1 is a master regulator of tau uptake and spread. *Nature*. 2020;580:381-385.

56. Gerson JE, Kayed R. Formation and propagation of tau oligomeric seeds. *Front Neurol*. 2013;4:93.

57. Hippensteel JA, Anderson BJ, Orfila JE, et al. Circulating heparan sulfate fragments mediate septic cognitive dysfunction. *J Clin Invest*. 2019;129:1779-1784.

58. Ely WE, Girard TD, Shintani AK, et al. Apolipoprotein E4 polymorphism as a genetic predisposition to delirium in critically ill patients. *Crit Care Med*. 2007;35:112-117.

59. Girard TD, Self WH, Edwards KM, et al. Long-term cognitive impairment after hospitalization for community-acquired pneumonia: a prospective cohort study. *J Gen Intern Med*. 2018;33:929-935.

60. Ehlenbach WJ, Hough CL, Crane PK, et al. Association between acute care and critical illness hospitalization and cognitive function in older adults. *JAMA*. 2010;303:763-770.

61. Herridge MS, Cheung AM, Tansey CM, et al. One-year outcomes in survivors of the acute respiratory distress syndrome. *N Engl J Med*. 2003;348:683-693.

62. Horwitz R, Maizes V. Integrative medicine and the long hauler syndrome-we meet again. *Am J Med*. 2020;134:418-419.

63. Huang C, Huang L, Wang Y, et al. 6-month consequences of COVID-19 in patients discharged from hospital: a cohort study. *Lancet*. 2021;397:220-232.

64. Siegelman JN. Reflections of a COVID-19 long hauler. *JAMA*. 2020;324:2031-2032.

SUPPORTING INFORMATION

Additional Supporting Information may be found online in the Supporting Information section.